

Article

Not peer-reviewed version

---

# Antituberculosis Propensity of Synthetic Biscoumarin Derivatives: An In Silico and In Vitro Approach

---

[Bashir A Sheikh](#) , [Basharat Ahmad Bhat](#) , Humaira Zareen , [Masood A Rizvi](#) <sup>\*</sup> , [Zahoor Ahmad](#) ,  
Mustfa Alkhanani , [Abdullah Almilaibary](#) , [Suliman A Alsagaby](#) , [Manzoor Ahmad Mir](#) <sup>\*</sup>

Posted Date: 29 March 2023

doi: 10.20944/preprints202303.0502.v1

Keywords: Tuberculosis; Biscoumarins; Ligand molecules; DprE1; Anti-tuberculosis activity; Molecular docking; MD Simulation; Cytotoxicity



Preprints.org is a free multidiscipline platform providing preprint service that is dedicated to making early versions of research outputs permanently available and citable. Preprints posted at Preprints.org appear in Web of Science, Crossref, Google Scholar, Scilit, Europe PMC.

Copyright: This is an open access article distributed under the Creative Commons Attribution License which permits unrestricted use, distribution, and reproduction in any medium, provided the original work is properly cited.

## Article

# Antituberculosis Propensity of Synthetic Biscoumarin Derivatives: An in Silico and In Vitro Approach

Bashir A Sheikh <sup>1</sup>, Basharat Ahmad Bhat <sup>1</sup>, Humaira Zareen <sup>2</sup>, Masood A Rizvi <sup>2\*</sup>, Zahoor Ahmad <sup>3</sup>, Mustfa Alkhanani <sup>4</sup>, Abdullah Almilaibary <sup>5</sup>, Suliman A. Alsagaby <sup>6</sup> and Manzoor A Mir <sup>1,\*</sup>

<sup>1</sup> Department of Bioresources, School of Biological Sciences, University of Kashmir, Srinagar-190006, India; email: sheikhashir198@gmail.com; basharatbhat.scholar@kashmiruniversity.net; drmanzoor@kashmiruniversity.ac.in

<sup>2</sup> Department of Chemistry, School of Physical & Mathematical Sciences, University of Kashmir, Srinagar-190006, India; email: masoodku2@gmail.com

<sup>3</sup> Clinical Microbiology PK/PD/ Laboratory, Indian Institute of Integrative Medicine (IIIM), Sanatnagar, Srinagar, J&K, India; email: zahooriiimap@gmail.com

<sup>4</sup> Department of Family and Community Medicine, Faculty of Medicine, Al Baha University, Albaha-65511, KSA; email: mkhanani@mcst.edu.sa

<sup>5</sup> Department of Biology, College of Science, Hafr Al Batin University of Hafr Al-Batin -31991, KSA; email: aalmilaibary@bu.edu.sa

<sup>6</sup> Department of Medical Laboratory Sciences, CAMS, Majmaah University, AL-Majmaah-11932, KSA; email: s.alsagaby@mu.edu.sa

\* Correspondence: masoodku2@gmail.com (M.A.R.); drmanzoor@kashmiruniversity.ac.in (M.A.M.)

**Abstract:** The concerning rise in emergence and prevalence of resistant strains to drugs of *M. tuberculosis* has prompted researchers to look for new and effective treatments. With this motive, biscoumarins were identified as the lead molecules on a whole-cell-based screening of several less explored low molecular weight bioactive compounds against *M. tuberculosis* strains. Among the screened biscoumarins, the highest dock score derivatives were synthesized (a-h) using a programmable microwave synthesizer for better yields and reaction control. The synthesized derivatives were evaluated against H37Rv, H37Ra, *M. smegmatis*, an MDR surrogate model, and other bacterial strains for the structure-activity response. Assessment of the synthesized library against mycobacterial strains led to the identification of compounds (f and d) as lead anti-tuberculosis agents. Compounds (f and d) exhibited less toxicity against human cell lines. At the same time, it displayed enjoyable activity wherein MIC concentrations were observed to be 16- and 32 µg/mL against the susceptible H37Rv, and H37Ra strains of *M. tuberculosis* and MIC value of 128 µg/mL for *M. smegmatis*, respectively. For mechanistic insights and identification of drug binding targets, molecular docking and dynamic simulations were employed for a panel of 16 mycobacterial enzymes essential for mycobacterial growth and survival. These in silico studies revealed the DprE1 enzyme as a druggable target for the anti-tuberculosis activity of the selected biscoumarins derivatives. Further investigation is underway in our laboratory, leading to its development as an anti-tuberculosis drug (animal model studies).

**Keywords:** tuberculosis; biscoumarins; ligand molecules; DprE1; anti-tuberculosis activity; molecular docking; MD simulation; cytotoxicity

## 1. Introduction

*Mycobacterium tuberculosis* (*Mtb*) is a bacterium responsible for developing tuberculosis infections in humans. Tuberculosis represents a highly contagious disease, se, a concerning global

health issue [1]. Annual TB mortality is estimated to be around 2 million. One-third of the global human population has tuberculosis in an asymptomatic latent state and is at higher risk for disease reactivation during its lifetime [2]. It is expected that 5–10% of people with latent tuberculosis (LTBI) may develop active tuberculosis (TB) in their lifetime, with the risk being higher in immune-compromised people such as those with acquired immunodeficiency syndrome (AIDS) [3–5]. Despite advancements in TB therapy, recurrence is still a big issue in developed countries [4,6]. In-depth research on tuberculosis over the last few decades has resulted in identifying new drug candidates currently undergoing pre-clinical and clinical studies. Because of their strong lipophilic nature, these medicines are potent *in vitro* but have poor *in vivo* pharmacokinetic characteristics. As a result, they are ineffective enough to meet the existing requirements for TB drug development [7,8]. TB drug development is currently focused on developing newer chemical moieties and therapeutic scaffolds that can increase pharmacological efficacy [7,9–11]. However, the new class of drugs challenges to meet the criterion for drug desirables, and the management of evolving resistant strains has become more difficult [5,11,12]. As a result, developing novel, potent drugs that meet the drug-likeness parameters is critical in the fight against serious illnesses and virulent pathogens. Currently, available anti-tuberculosis treatment for *M. tuberculosis* has several drawbacks, including toxicity and the need for extended therapy [13–15]. As a result, there is an immediate need for tuberculosis therapeutics that are both more reliable and associated with fewer adverse effects (TB). As a result, medicinal plants could be a viable option for combating tuberculosis. Alternatives to standard tuberculosis treatment include plant metabolites with high therapeutic promise [8]. Natural compounds are essential for discovering and developing novel antiviral, antibacterial, and anticancer chemical entities as they possess the properties of substantial bioavailability and most minor side effects. Natural antibiotics encompass the secondary metabolites released by microorganisms, which essentially stop the growth of bacteria by specifically targeting some of the cell's essential processes, which may include cell wall biosynthesis, RNA/DNA, as well as proteins. D[16]. Natural products derived from secondary metabolites of medicinal plants contain a variety of fascinating therapeutic qualities, including antimycobacterial activity; thus, natural derivatives and their synthetic analogs could be promising for finding new anti-TB leads [17].

Benzene rings fused to six-membered lactone rings form coumarins, an oxygen heterocycle compound. Many fungal species convert coumarin into dicoumarol natural anticoagulant, and vitamin K antagonist. Dicoumarol is a potential antimicrobial entity, and it is chemically represented as [3,3'-methylenebisphenol] (4-hydroxy-2H-chromen-2-one) (**Scheme 1**). Biscoumarins have a dicoumarol-type ring system that can be produced by reacting 4-hydroxycoumarin with different aldehydes [18].

The biological activities of compounds with a biscoumarin scaffold encompass inhibiting enzymes and antibacterial, antifungal, anthelmintic, antiviral, and insecticidal activity [19]. Additionally, biscoumarins are believed to have anti-inflammatory, hypnotic, and spasmolytic effects [20,21]. Further, it has been stated that biscoumarins are anti-HIV compounds that act against HIV-1 integrase [22]. Functionalized biscoumarin structures have attracted attention in the pharmaceutical area because of their wide structural diversity, capacity to scavenge microorganisms, modulated lipophilicity for bioavailability and intriguing pharmacokinetic features [23]. Biscoumarins can also make hydrogen bonds because they possess the hydroxyl groups in their structure. Including the halogen group, particularly fluorine and bromine substituents, into the biscoumarin moiety increases its lipophilicity for efficient bacterial cell membrane permeability [24]. As a result, it becomes a crucial metric for cell permeability while studying antimicrobial propensity [25].

Inspired by all the parameters mentioned above, in the present study, biscoumarins were chosen as the target entities against different mycobacterial strains, including *H37Ra*, *H37Rv* strain, and *M. smegmatis*, among other bacterial strains (through broth dilution method), because of their structural diversity, increased potency, and ease in synthesis. From the drug compatibility point of view, the molecules were also screened for their toxic effect on several human cell lines. A molecular docking correlation to investigate the binding affinity of the selected biscoumarins with drug target Decaprenylphosphoryl-β-d ribose 2'-epimerase (DprE1) (with PDB-ID 4FEH), an essential enzyme

involved in the biosynthesis of the cell wall, that displays its vital contribution in the synthesis of arabinogalactan and lipoarabinomannan was also carried out. s.

## 2. Methods and materials

During the current study, Merck (India) supplied the chemicals required for synthesis. Reaction monitoring was performed over TLC Silica gel 60F Aluminium sheets using a hexane-ethyl acetate (8:2) solvent system, and the reaction spots were located in a UV chamber under both short (254 nm) and long (365 nm) UV light. Perkin Elmer 2400 Series II CHN Elemental Analyzer was used for elemental analyses. Infrared spectra were obtained on a Perkin Elmer-Spectrum RX-FTIR instrument.  $^1\text{H}$  NMR spectra were obtained using  $\text{CDCl}_3/\text{DMSO}-d_6$  as solvent and tetramethylsilane (TMS) as internal standard over a Bruker Avance II 400 MHz NMR Spectrometer. Mass Spectra were obtained on Waters Micromass Q-ToF Micro instrument. A programmable microwave synthesizer (Anton Paar mono wave 300) was used for microwave-assisted synthesis [26]. Perfit melting point apparatus was used to take the melting points in open capillaries.

### 2.1. Procedure for the synthesis of Bis (4-hydroxy-2H-chromen-2-ones) a-h (refluxing conditions)

Aldehydes (2mmol) and 4-hydroxycoumarin (**I**) (0.648g,4mmol) with a 1:2 molar ratio mixture in a 2:1 water-ethanol mixture were refluxed in the round-bottomed flask (25 mL) over a water bath at  $70^\circ\text{C}$ . Thin-layer chromatography was used to monitor the progress of the reaction for 3 hours periodically. As the TLC evidenced the completion of the reaction process, the mixture of the reaction was soon cooled down to the room temperature and filtered under suction. The ethanol-washed residue was then dried as a crude sample. Re-crystallization from the ethanol chloroform (7:3) mixture allowed for the purification of the crude sample.

### 2.2. Synthesis of Bis(4-hydroxy-2H-chromen-2-ones) a-h through Method A

4-hydroxycoumarin (0.648g,4mmol) and selected aldehydes (2mmol) were added to 3.5 mL of the 2:1 v/v water-ethanol system. A domestic microwave oven irradiated this mixture after sealing it in a Teflon tube. A series of heating-cooling cycles were programmed into the microwave heating of the reaction mixture to prevent pressure build-up until the reaction period was complete. To mitigate pressure build-up and overheating, a 30-second irradiation period at an average power of 1000W was preceded by a two-minute rest period. The heating-cooling cycles continued until the reaction was completed, as indicated by TLC. After the reaction's completion, the mixture was brought up to room temperature, and the end product was suction-filtered, ethanol-washed, and air-dried. .

### 2.3. Synthesis of Bis(4-hydroxy-2H-chromen-2-ones) through Method B

A reaction mixture comprising aldehydes (2 mmol) and 4-hydroxycoumarin (4 mmol) in 4 mL of ethanol solvent were mixed in a 10 mL borosilicate glass vial (G10) sealed with a PTFE-coated silicone septum snap cap. This reaction mixture was irradiated in a microwave synthesizer under controlled conditions of  $150^\circ\text{C}$  at 600 rpm stirring speed for the optimized 3 min hold time. The cooling temperature of  $55^\circ\text{C}$  was set for reactions before the start of the next cycle. After completion of the reaction, the product was filtered, washed with ethanol, and dried. The crude product was re-crystallized from ethanol to obtain a percent yield. The desired compounds were characterized spectroscopically using FTIR,  $^1\text{H}$  NMR, and  $^{13}\text{C}$  NMR.

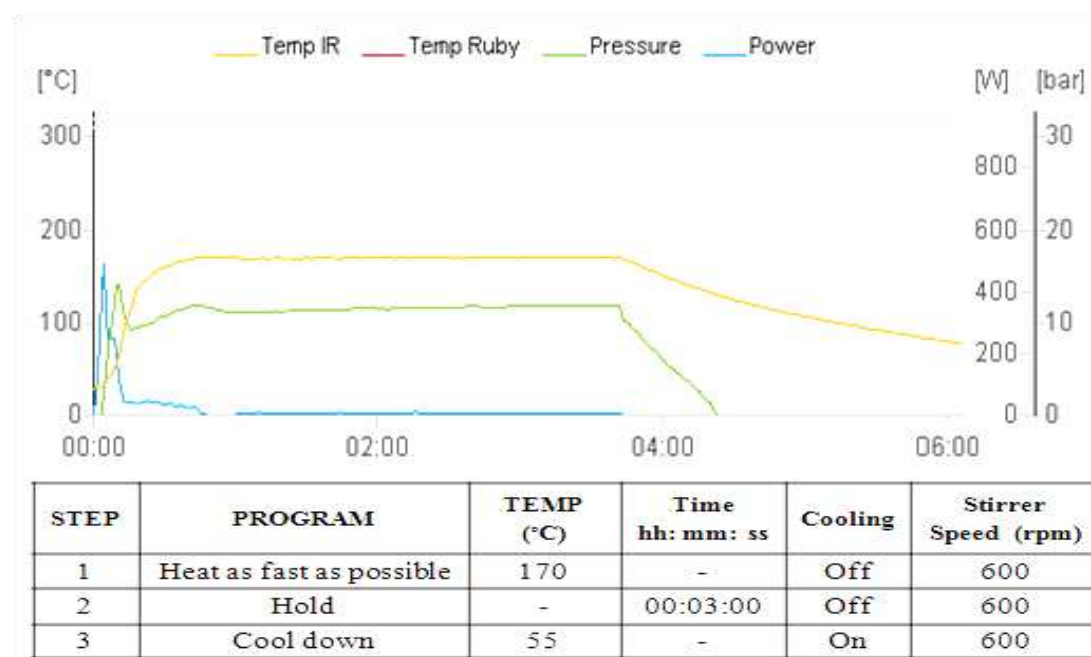


**Figure 1.** The microwave irradiation program for the biscoumarin synthesis under catalyst-free aqueous phase in Anton Paar Monowave 300 Synthesizer.

#### 2.4. Antibacterial activity spectrum of biscoumarin

##### • Drugs, chemicals, and media

Drugs including levofloxacin (LVX), isoniazid (INH), ethambutol (EMB), rifampicin (RIF), amikacin (AMK), and ciprofloxacin (CIP) were procured from the USA based Sigma-Aldrich platform. Media like 7H9 broth, 7H11 agar, Muller Hinton Broth (MHB), Muller Hinton agar (MHA), and supplements including ADC and OADC were procured from HI Media (India) Merck (India) platform was chosen to procure Tween 80 detergent. Thermo Fisher Scientific, Waltham, MA, the United States, provided the penicillin-streptomycin, Dulbecco's Modified Eagle's Medium (DMEM), and fetal bovine serum (FBS) for experimentation purposes.

The National Centre for Cell Science (NCCS) in Pune provided the cell lines, including M.D.Anderson-Metastatic Breast-231 (MDA-MB-231) Michigan Cancer Foundation-7 (MCF-7), and human embryonic kidney cells-293 (HEK-293) for use in the current study. Furthermore, the test compound stock solution was prepared separately using dimethyl sulfoxide (DMSO), wherein different solvents were used for other standard or control drugs. Methanol was used as a solvent for RIF, Milli-Q water was used as a solvent for LVX and INH, and all the prepared solutions were kept at -20°C. At the time of experimentation, fresh preparation of working solution was carried out using Middlebrook 7H9 broth for anti-TB agents. For other antibacterial agents, Muller Hinton Broth was used accordingly.

##### • Bacterial strains, compound dissolving, and dilution

The microorganisms used in this study were procured from Hi-Media (India), of which 2 were Gram-positives: *B. subtilis* (ATCC 6633), *E. faecalis* (ATCC 29212), and Gram-negative, *P. aeruginosa* (ATCC 9027) and *Escherichia coli* (ATCC 11105). Glycerol stocks of these strains were prepared in Müller Hinton Broth (MHB) supplemented with 10% (v/v) glycerol at -20°C and were routinely cultured in MHB. *M. tuberculosis* H37Rv (ATCC 27294), *M. tuberculosis* H37Ra (ATCC 25177), and *M. smegmatis* (ATCC 607-0114P) were obtained from American Type Culture Collection (USA). Gram-negative and gram-positive bacterial cultures were kept in a bacterial incubator at 37°C for balanced growth. This was followed by the preparation of 1mL aliquots using glycerol (40%) in the 1:1 ratio were kept in the freezer for future use at -20 °C. On the other hand, the sub-culturing of bacterial cultures of *mycobacterial* strains was also carried out. Middlebrook 7H9 broth enriched with ADC (Albumin, Dextrose, and Catalase) was used to grow mycobacterial strains to 10<sup>8</sup> CFU/mL cell



density. Subsequently, glycerol stocks of different strains were prepared and stored at -20°C in 1.0 mL aliquots. To achieve a concentration of 1000 µg/mL, compounds (10 mg) were dissolved in 10 mL DMSO. Utilizing media, the working concentration of 128 µg/mL was prepared.

- **Determination of minimum inhibitory concentration (MIC) against Mycobacterial strains**

The conventional broth dilution method was applied to calculate the MIC for the strains of *mycobacteria*. Drug stock solutions were dissolved in Middlebrook 7H9 broth (consisting of 10%ADC) in the absence of Tween 80. Drug solutions were made in 96-well plates (Nest Biotech, China), employing two-fold serial dilutions so that the test compounds concentrations ranged from 0.125 to 128 µg/mL while maintaining a growth and media control column (200 µl in each well) [27]. Except for the media control column, an equivalent volume (50 µl) of bacterial inoculum comprising mid-log phase growing *M. tuberculosis* was added so that the final cell density in each well equals approximately 1x10<sup>5</sup> CFU/mL. After three weeks of incubation at 37°C, the plates were visually inspected, and the results were recorded. Minimum inhibitory concentration was considered the lowest molecule concentration that suppressed the observable bacterial growth. Positive controls for mycobacterial strains included isoniazid, ethambutol, and levofloxacin. The negative control for mycobacterial species was drug-free broth and the incubation period was for seven days at 37°C. The experiments were carried out three times (in triplicates). A similar verification process was carried out for mycobacterial inoculums by plating a 10-fold dilution of the sample on Middlebrook 7H11 agar plates that had been supplied with OADC (oleic acid, albumin, dextrose, and Catalase). The plates were incubated at 37°C for four weeks and the results read. [27].

- **Determination of (MIC) against gram-positive and gram-negative bacteria**

In a 96-well microplate, dilution of compounds was performed in geometrically increasing concentrations (0.25 µg/mL to 128 µg/mL) with 200 µL of liquid growth medium. The inoculum was prepared to contain 10<sup>5</sup> CFU/mL of bacterial culture in 50 µL. As a positive control, levofloxacin was utilized for both gram-negative and gram-positive microbial strains. For gram-positive and gram-negative bacteria, the presence of turbidity or sediment after 24 hours of incubation at 37°C indicates the growth of microorganisms. The MIC was calculated based on the concentration of no turbidity. Original CFU for gram-positive and gram-negative bacterial strains was determined by plating serial 10-fold dilutions of the inoculum onto the nutrient agar plates kept at 37°C for 24 Hours [28].

## 2.5. Cytotoxicity assay

MCF-7, MDA-MB-231, HEK-293, and 4T1 cell lines were used in the present study to check the toxicity of compounds. Prof Annapoorni Rangarajan, IISC, Bangalore, kindly supplied the 4T1 cell line. Regularly, the identification of these cells was confirmed using cell morphology. DMEM was used to culture cells. 10% fetal bovine serum (FBS) and 1% penicillin-streptomycin were added to the medium. The cells were cultured in a CO<sub>2</sub> incubator (5%) at 37°C. MTT (dimethylthiazol-diphenyltetrazolium bromide) assay was performed to analyze the cytotoxicity of compounds in *in vitro* human models. Cells were seeded in 96 well plates at 3000 x 10<sup>3</sup> cells/well. Next, the cells were treated with a single dose of 50 µM of compounds in four replicates. The test compounds were freshly prepared and treated for 72 hrs. The medium was replaced with MTT solution (Vybrant MTT cell proliferation assay kit Invitrogen) after 72 hours of incubation, and each well's absorption was assessed at 490 nm. Graph Pad software (version 8) was utilized to calculate cell viability and cytotoxicity, as well as plot graphs.

## 2.6. Molecular docking and MD simulation studies

- **Molecular Docking**

This work aimed to insight into the binding properties of the ligand with DprE1 (PDB ID: 4FEH) protein using geometrically optimized ligand (f). Protein was further vetted for missing side-chain residues using the open Molecular Mechanics (MM) simulation program (<https://openmm.org/>) before being used in molecular interaction investigations. Auto dock v 4.2.6 was used for molecular docking investigations[30]. the binding cavity was determined by using the co-crystallized X-

ray structure of the DprE1 protein from the RCSB PDB. The positions of residues within three spaces of the co-crystallized ligand were calculated. The energy was reduced following cavity selection using the steepest descent and conjugate gradient algorithms. The energy was reduced following cavity selection using the steepest descent and conjugate gradient algorithms. After putting the nonpolar hydrogens together, the receptor and target molecules were saved in pdbqt format. Grid boxes were made with a space of 0.3 between them. Docking experiments of the protein-ligand complex were conducted using the Lamarckian Genetic Algorithm (LGA) to determine the lowest free energy of binding (G). [30]. Experiments with molecular modeling were carried out three times with the same default settings for parameters such as the number of solutions (50 in each experiment), the number of evaluations (2,500,000), and the maximum number of generations (2,700), among other settings. The Root Mean Square Deviation (RMSD) clustering maps were produced following docking by re-clustering with clustering tolerances of 0.25, 0.5, and 1 to find the optimal cluster with the lowest energy score and the higher number of populations, respectively.

- **Molecular dynamics simulation (MD)**

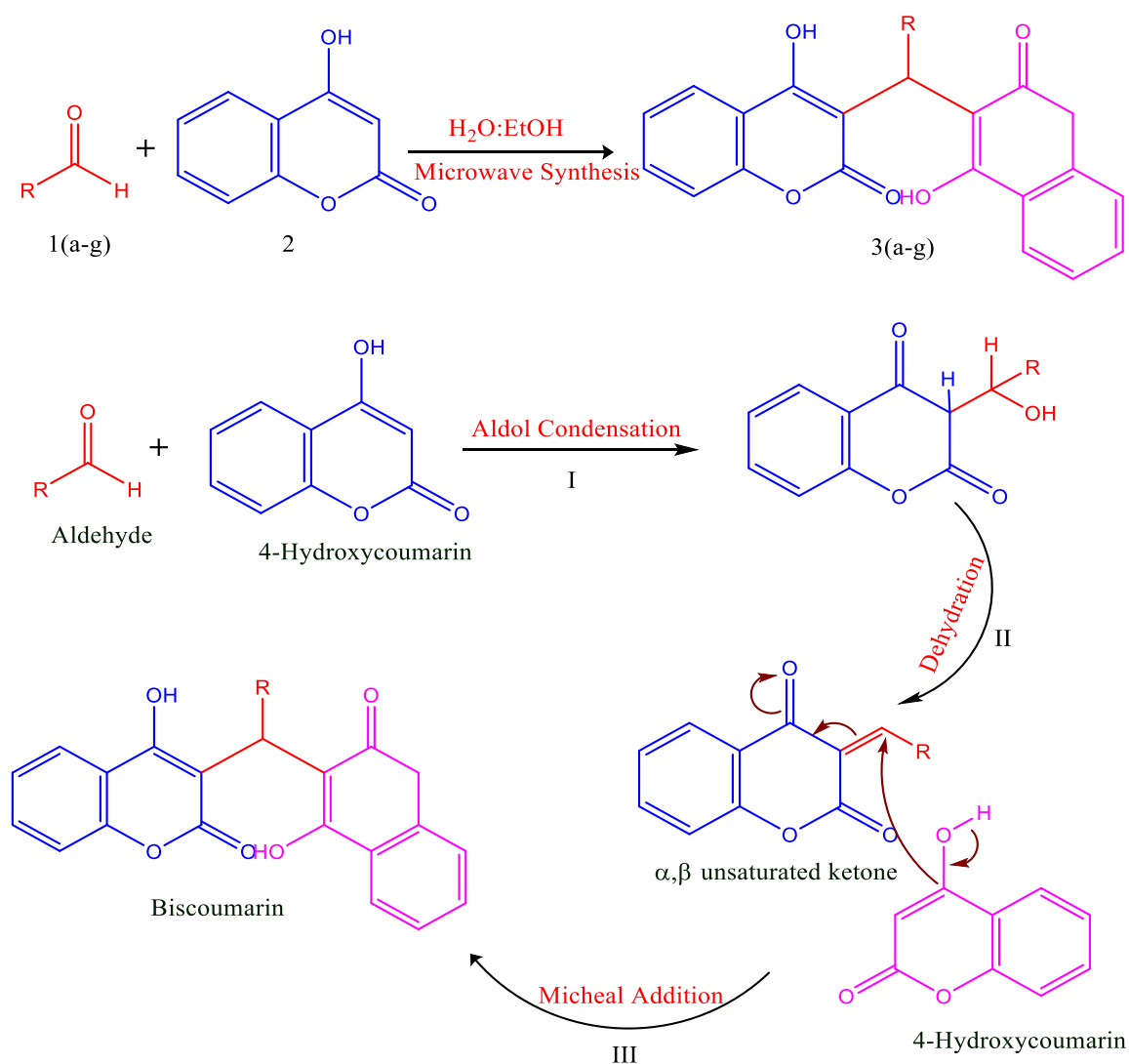
The Desmond 2020.1 from Schrodinger LLC was used for the MD simulation studies on the docked complexes for DprE1 with Compound (f). This system used the OPLS-2005 force field and the explicit solvent model with the SPC water molecules [31–33]. To simulate the physiological environment, NaCl solutions were added to the system along with Na<sup>+</sup> ions to neutralize the charge of 0.15 M. To retrain the system over the protein-ligand complexes, the system was initially equilibrated using an NVT ensemble for 15 ns. An NPT ensemble was used to complete a brief run of equilibration and minimization for 20 ns following the previous step. The NPT ensemble was established utilizing the Nose-Hoover coupling scheme, with the temperature at 37 °C, the pressure at 1 bar, and the relaxation time at 5.0 ps. being kept constant throughout all simulations [34]. A 2fs time step was also utilized. The pressure was controlled using the Martyna-Tuckerman-Klein chain coupling scheme barostat method with a relaxation time of 2 ps [34]. Long-range electrostatic interactions were calculated using the particle mesh Ewald method, and the Coulomb interaction radius was set at 9 Å [35]. The bonded forces were calculated for each trajectory using the RESPA integrator for a time step of 2 fs.

Calculations were performed to determine the Root Mean Square Fluctuation (RMSF), Root Mean Square Deviation (RMSD), the number of hydrogen bonds (H-bonds), the Radius of gyration (Rg), and the Solvent Accessible Surface Area (SASA). All of these variables were used to evaluate the stability of the MD simulations.

### 3. Results

#### 3.1. Chemistry/Synthesis

4-hydroxycoumarin (1) on reaction with various aldehydes (a-h) leads to the formation of desired products either in minimal yield or no product formation under the pure water and catalyst-free conditions due to limited reactant solubility. Therefore, using an aqueous ethanol solvent system was used to increase the yield as the required reactants have appreciable solubility in ethanol. For optimization, 4-hydroxycoumarin (1) and benzaldehyde (a) were initially reacted under different H<sub>2</sub>O: EtOH system concentrations and refluxed for 9 hours. It was observed that on reacting the 4-hydroxycoumarin (1) with benzaldehyde in a 2:1 molar ratio in the solvent system, H<sub>2</sub>O: EtOH in a 2:1 ratio increases the product yield significantly (**Scheme I**). Employing these optimized reaction conditions, 4-hydroxycoumarin (2) was reacted with other aldehydes (b-h), and a library of biscoumarins was prepared in appreciable yield (**Figure 2**).



Scheme I. Synthesis of biscoumarins.



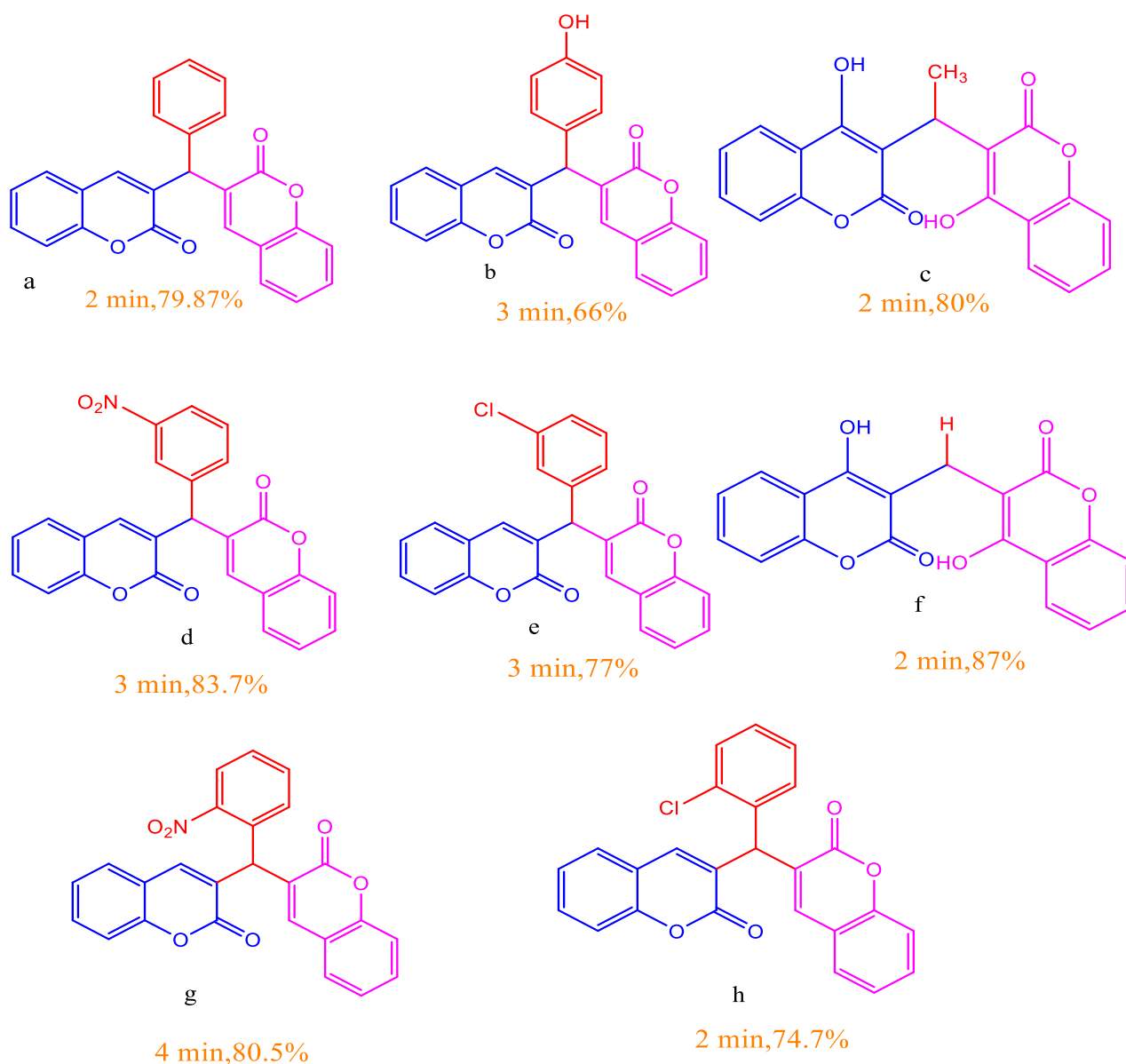


**Figure 2.** A library of eight biscoumarin motifs with their time and % yield.

**3,3'-(Phenyl-methylene) bis(2H-chromen-2-one) (a);** mp: 229–231 °C; light cream solid; IR spectrum (KBr),  $\nu/\text{cm}^{-1}$ : 757 (C-H out of plane bending vibrations of benzene ring), 1566, 1496, 1450 (C=C stretching of aromatic ring), 1654, 1618 (C=O stretching of lactone ring of coumarin), 3064, 3023 (O-H stretching);  $^1\text{H}$  NMR spectrum (400MHz,  $\text{CDCl}_3$ )  $\delta$  (ppm): 11.53 (s, 1H, OH), 11.30 (s, 1H, OH), 7.20–8.07 (m, 13H, Ar-H), 6.09 (s, 1H, CH);  $^{13}\text{C}$  NMR (100 MHz,  $\text{CDCl}_3$ )  $\delta$  (ppm): 56.8, 116.1, 120.2, 125.4, 126.3, 127.7, 127.9, 128.6, 140.8, 144.4, 153, 161.9; ESI-MS for  $\text{C}_{25}\text{H}_{16}\text{O}_6$  calculated: 410.3, found: 410.9.

**3,3'-((4-Hydroxyphenyl) methylene) bis (2H-chromen-2-one) (b);** mp: 207–210 °C; White crystalline solid; IR spectrum (KBr),  $\nu/\text{cm}^{-1}$ : 3020, 3076, 3356 (O-H), 1616, 1648 (C=O), 1441, 1512, 1565 (C=C), 762 (C-H);  $^1\text{H}$  NMR spectrum (400MHz,  $\text{CDCl}_3$ )  $\delta$  (ppm): 11.45 (2H, s, OH), 6.74–8.03 (13H, m, H Ar), 6.01 (1H, s, CH);  $^{13}\text{C}$  NMR (100 MHz,  $\text{CDCl}_3$ )  $\delta$  (ppm): 56.8, 116.1, 120.2, 125.4, 126.3, 127.9, 128.3, 130.4, 137, 140.8, 153.9, 155.5, 161.9; ESI-MS for  $\text{C}_{25}\text{H}_{14}\text{O}_7$  calculated: 426.3, found: 426.9.

**3,3'-(Ethane-1,1-diyl)bis(4-hydroxy-2H-chromen-2-one) (c);** mp: 225–228 °C; White crystalline solid; IR spectrum (KBr),  $\nu/\text{cm}^{-1}$ : 3062 (O-H), 2800, 2904 (C-H), 1599, 1639 (C=O), 1453, 1501 (C=C), 769, 750 (C-H);  $^1\text{H}$  NMR spectrum (400MHz,  $\text{CDCl}_3$ )  $\delta$  (ppm): 11.20 (2H, s, OH), 7.39–7.95 (8H, m, H Ar), 3.82 (2H, s,  $\text{CH}_2$ );  $^{13}\text{C}$  NMR (100 MHz,  $\text{CDCl}_3$ )  $\delta$  (ppm): 11.2, 23.5, 103.8, 116.4, 123.3, 125.4, 128, 152.5, 162, 167; ESI-MS ( $m/z$ ) for  $\text{C}_{19}\text{H}_{10}\text{O}_6$  calculated: 351.2, found: 350.33.

**3,3'-((3-Nitrophenyl)methylene)bis(2H-chromen-2-one) (d);** mp: 230 °C; Light yellow crystalline solid; IR spectrum (KBr),  $\nu/\text{cm}^{-1}$ : 3022, 3077 (O–H), 1610, 1663 (C=O), 1449, 1496, 1566 (C=C), 1347, 1530 (NO<sub>2</sub>), 764 (C–H); <sup>1</sup>H NMR spectrum (400MHz, CDCl<sub>3</sub>)  $\delta$  (ppm): 8.86 (2H, s, OH), 7.34–8.08 (12H, m, H Ar), 6.58 (1H, s, CH); <sup>13</sup>C NMR (100 MHz, CDCl<sub>3</sub>)  $\delta$  (ppm): 55.8, 120.2, 120.9, 121.1, 121.8, 126.3, 127.9, 128.3, 134.2, 140.8, 145.2, 147.9, 153, 161.9; ESI-MS (m/z) for C<sub>25</sub>H<sub>13</sub>NO<sub>8</sub> calculated: 455.3, found: 455.9.

**3,3'-((3-Chlorophenyl)methylene)bis(2H-chromen-2-one) (e);** mp: 220–224 °C; White crystalline solid; IR spectrum (KBr),  $\nu/\text{cm}^{-1}$ : 3019, 3074 (O–H), 1617, 1658 (C=O), 1452, 1496, 1568 (C=C), 761 (C–H), 651 (C–Cl); <sup>1</sup>H NMR spectrum (400MHz, CDCl<sub>3</sub>)  $\delta$  (ppm): 11.57 (1H, s, OH), 11.30 (1H, s, OH), 7.09–8.07 (12H, m, H Ar), 6.04 (1H, s, CH); <sup>13</sup>C NMR (100 MHz, CDCl<sub>3</sub>)  $\delta$  (ppm): 56.3, 116.1, 120.2, 125.4, 125.8, 128.3, 130, 134.2, 140.8, 143.6, 153, 161.9; ESI-MS (m/z) for C<sub>25</sub>H<sub>13</sub>ClO<sub>6</sub> calculated: 444.8, found: 444.9.

**3,3'-Methylenebis(4-hydroxy-2H-chromen-2-one) (f);** mp: 275–279 °C; White crystalline solid; IR spectrum (KBr),  $\nu/\text{cm}^{-1}$ : 3062 (O–H), 2800, 2904 (C–H), 1599, 1639 (C=O), 1453, 1501 (C=C), 769, 750 (C–H); <sup>1</sup>H NMR spectrum (400MHz, CDCl<sub>3</sub>)  $\delta$  (ppm): 8.20 (2H, s, OH), 7.33–7.95 (8H, m, H Ar), 3.82 (2H, s, CH<sub>2</sub>); <sup>13</sup>C NMR (100 MHz, CDCl<sub>3</sub>)  $\delta$  (ppm): 18.7, 110.2, 116.4, 123.4, 125.4, 128.3, 152.5, 160.8, 169.6; ESI-MS (m/z) for C<sub>25</sub>H<sub>13</sub>ClO<sub>6</sub> calculated: 334.2, found: 334.8.

**3,3'-((2-Nitrophenyl)methylene)bis(2H-chromen-2-one) (g);** mp: 194–197 °C; Light yellow crystalline solid; IR spectrum (KBr),  $\nu/\text{cm}^{-1}$ : 3022, 3078 (O–H), 1616, 1655 (C=O), 1454, 1495, 1565 (C=C), 1352, 1525 (NO<sub>2</sub>), 763 (C–H); <sup>1</sup>H NMR spectrum (400MHz, CDCl<sub>3</sub>)  $\delta$  (ppm): 8.18 (2H, s, OH); 7.17–7.95 (12H, m, H Ar), 6.71 (1H, s, CH); <sup>13</sup>C NMR (100 MHz, CDCl<sub>3</sub>)  $\delta$  (ppm): 52.2, 116.1, 120.2, 125.4, 126.3, 126.9, 128.3, 130.4, 134.6, 140.8, 147.8, 153.9, 161.9, ESI-MS (m/z) for C<sub>25</sub>H<sub>13</sub>NO<sub>8</sub> calculated: 455.3, found: 455.9.

**3,3'-((2-chlorophenyl)methylene)bis(2H-chromen-2-one) (h);** mp: 197–199 °C; White crystalline solid; IR spectrum (KBr),  $\nu/\text{cm}^{-1}$ : 2981, 3072 (O–H), 1617, 1646 (C=O), 1451, 1496, 1564 (C=C), 761 (C–H), 641 (C–Cl); <sup>1</sup>H NMR spectrum (400MHz, CDCl<sub>3</sub>)  $\delta$  (ppm): 11.63 (1H, s, OH), 10.93 (1H, s, OH), 7.21–8.03 (12H, m, H Ar), 6.14 (1H, s, CH); <sup>13</sup>C NMR (100 MHz, CDCl<sub>3</sub>)  $\delta$  (ppm): 51.7, 116.1, 120.2, 125.4, 125.8, 126.9, 127.7, 128.3, 128.7, 131.2, 140.8, 143.6, 153, 161.9; ESI-MS (m/z) for C<sub>25</sub>H<sub>13</sub>ClO<sub>6</sub> calculated: 444.8, found: 444.9.

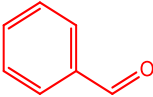
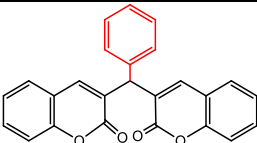
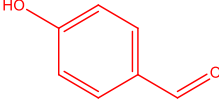
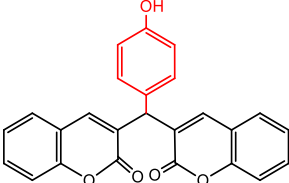
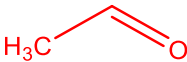
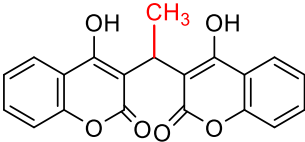
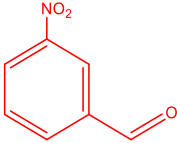
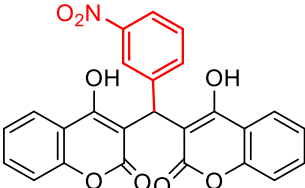
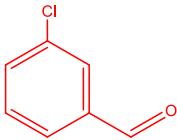
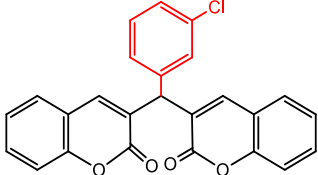
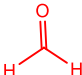
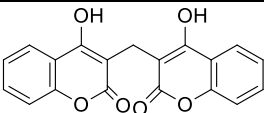
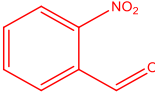
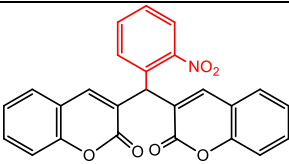
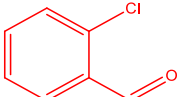
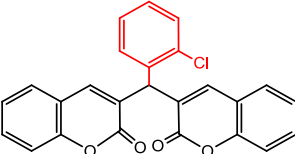
### 3.2. Antibacterial activity spectrum of biscoumarin

#### • The anti-tuberculosis activity of compounds

To evaluate the *in vitro* efficacy and the anti-tuberculosis potential of a series of compounds, they were surveyed against various strains of mycobacteria, including the standard H37Rv, and H37Ra strains of *M. tuberculosis* and *M. smegmatis*, a surrogate MDR model. The series showed a similar activity spectrum as with the avirulent strain of *Mtb* (H37Ra). Compound (f) was most active in the series with MIC value 16  $\mu\text{g/mL}$  [36]. The compound (f) exhibited the best activity against the virulent *M. tuberculosis* (H37Rv) with MIC values of 16  $\mu\text{g/mL}$ . This MIC value was followed by the compound (d) with 32  $\mu\text{g/mL}$ . The other compounds showed activity at MIC 64  $\mu\text{g/mL}$  against H37Ra and H37Rv strains. The series of compounds were active against *M. smegmatis*, the surrogate screen of MDR-TB at higher concentrations with a MIC value of 128  $\mu\text{g/mL}$ . These compounds were active against these panels of microbes at varied concentrations. Results revealed that compound (f) was the most active compound at the concentration of 16  $\mu\text{g/mL}$  [36], followed by compound (d) with the MIC value of 32  $\mu\text{g/mL}$  against *Mtb*.

In contrast, other series compounds were active at the concentration of 32–64  $\mu\text{g/mL}$  against virulent and avirulent strains of *Mtb*, which is regarded as significant owing to their low cytotoxicity effect. However, after the *in vitro* screening, two compounds (a and c) were not active against any mycobacterial strain; if active at significantly higher concentrations, these two compounds were not carried out for further investigations. (Table 1).

**Table 1.** A comparative account of the Biscoumarin synthesis under conventional refluxing and microwave irradiation.

Aldehyde	Product	Refluxing (2:1 v/v) H <sub>2</sub> O: EtOH		Microwave (2:1 v/v) H <sub>2</sub> O: EtOH	
		Time (hrs)	Yield (%)	Time (min)	Yield (%)
Benzaldehyde 		12	75.24	2.5	79.00
<i>p</i> -Hydroxybenzaldehyde 		24	64.95	3	65.65
Acetaldehyde 		3	79	2	80
<i>m</i> -Nitrobenzaldehyde 		4	80	3	83.7
<i>m</i> -Chlorobenzaldehyde 		2	92.72	2	78.94
Formaldehyde 		4	81.84	2	86.45
<i>o</i> -Nitrobenzaldehyde 		7	76.80	2.5	83.15
<i>o</i> -Chlorobenzaldehyde 		13	84.54	3	77.26

• **Determination of MIC against gram-positive and gram-negative bacterial strains**

The synthesized biscoumarins were then evaluated for their antimicrobial activity upon various representative gram-positive and gram-negative bacteria, such as *E. coli*, *E. faecalis*, *B. subtilis*, and *Pseudomonas aeruginosa*. The moderate activity of compounds was observed against bacteria *E. faecalis*, *P. aeruginosa*, and *E. coli*, with MIC values of 64-128µg/mL. At the same time, the compounds exhibited good activity against *B. subtilis* with a MIC value of 64 µg/mL[37]. But in accordance with anti-TB evaluation, two compounds (a and c) did not display any activity against

these gram-negative and gram-positive strains. Therefore, the MIC value of compounds of the series against different bacterial strains was very high, ranging from  $\geq 128 \mu\text{g/mL}$ , which indicates that the compounds show much more good MIC values against the mycobacterial strains rather than other bacterial strains; hence, an essential parameter for the anti-tuberculosis drug discovery process.

Wherein INH, ETB, and LVX represent the isoniazid, ethambutol, and levofloxacin, which are standard antibacterial drugs approved by FDA.

### 3.3. Compound cytotoxicity

The ability of a molecule to differentiate between bacterial and mammalian cells is one of the most crucial aspects of the drug discovery process. This ability allows the molecule's activity and toxicity to be distinguished. [37]. Therefore, using the MTT cell viability assay, we investigated the compound's cytotoxicity against the human embryonic cell line 293 (HEK-293) and three other cell lines (MCF-7, MDA-MB-231, and 4T1). At a concentration of  $50 \mu\text{M}$ , it was noted that none of the compounds significantly affected the growth of any of the four cell lines (about  $<30\%$  growth inhibition). **Table 2** displays the outcomes at  $50 \mu\text{M}$  for all the chemicals against the four cell lines. Compounds (e) and (h) showed more than  $30\%$  growth inhibition in 4T1 cells. At this concentration, all the compounds inhibited cell growth by  $<50\%$  in all the tested cell lines. At a concentration of  $50 \mu\text{M}$ , compounds b and f, deemed the best leads, were found to be non-toxic to all of the cell lines that were evaluated, exhibiting an inhibition of  $<20\%$ .

**Table 2.** Antibacterial activity evaluation of biscoumarins through broth microdilution method.

S. No	Compound	<i>E. coli</i>	<i>E. faecalis</i>	<i>B. subtilis</i>	<i>P. aeruginosa</i>	<i>Mtb H37 Rv</i>	<i>Mtb H37Ra</i>	<i>M. smegmatis</i>
1	b	128	128	64	128	64	64	128
2	d	128	128	64	128	32	32	128
3	e	128	128	64	128	64	64	128
4	f	128	64	64	128	16	16	128
5	g	128	128	64	128	64	64	128
6	h	128	128	64	128	64	64	128
	INH	NA	NA	NA	NA	0.325	0.325	1.25
	ETB	NA	NA	NA	NA	1.25	1.25	0.039
	LVX	0.031	0.156	0.125	0.078	0.15	0.15	0.039

Given that their MIC ranged from  $16\text{--}128 \mu\text{g/mL}$  against various mycobacterial strains and that they have no effect on human cells even at concentrations of  $50 \mu\text{M}$ , these chemical entities have a therapeutic index that is remarkably suited and deserves *in vivo* testing. In conclusion, the present study describes synthesizing and evaluating a series of biscoumarin molecules (a-h) against mycobacterial strains. This study identified biscoumarin molecules as anti-TB agents in general and (f and d) as potential lead molecules whose MIC falls close to standard anti-TB drugs. Further, the activity of most of these molecules is highly selective against virulent and avirulent strains of *M. tuberculosis* compared to other microbes. These also proved to be non-toxic to human cell lines.

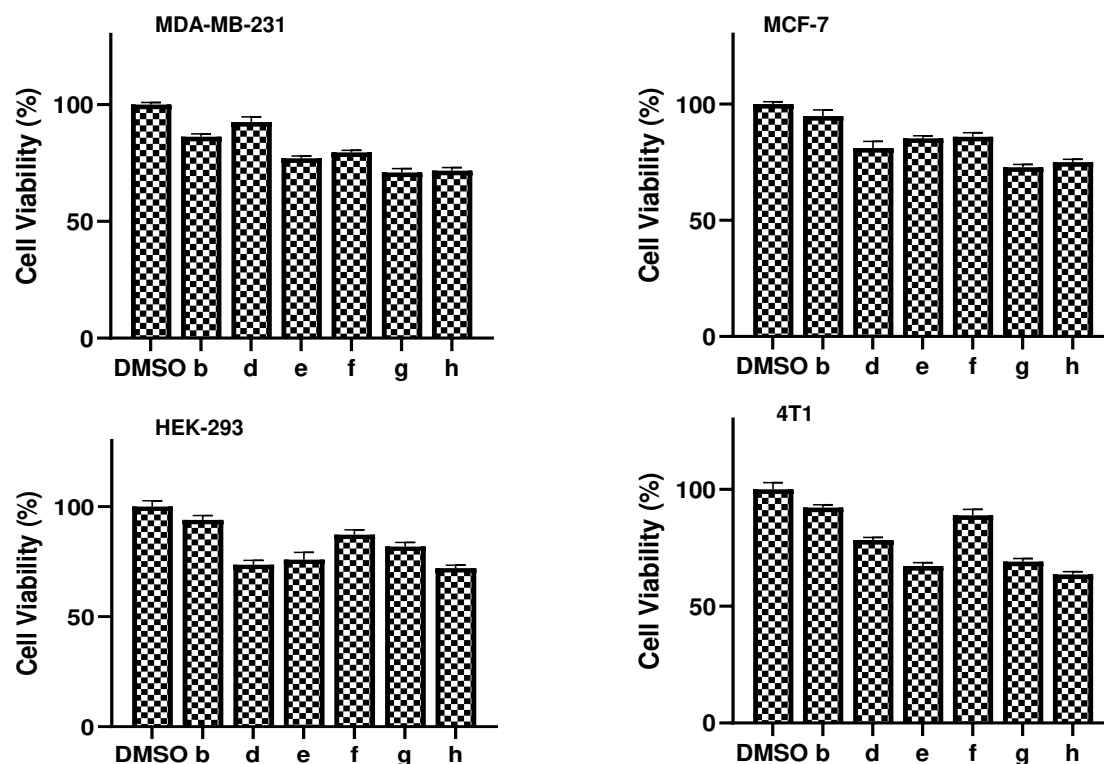


**Figure 3.** Cell viability assay of four cell lines treated with 50µM of biscoumarins (a-h) and DMSO as control.

### 3.4. Molecular Docking

Most binding energy scores (95%) are derived from the cluster with the lowest RMSD, 0.25 Å, based on the best cluster. With the lowest binding energy ( $\Delta G$  – 9.3 kcal/mol) and inhibitory concentration,  $K_i$  (0.4 µM), Compound (f) showed a considerable binding affinity for the DprE1 (**Figure 4A**). His 132 and Lys418 residues at the protein binding cavity engaged in conventional hydrogen bonding when the ligand (f) interacted with it. In addition to hydrogen bonds, the ligand and amino acid residues interacted non-covalently through interactions like Vander Waal's interactions and Pi-alkyl interactions with Pro116, Ile131, and Lys134. (**Figure 4**).

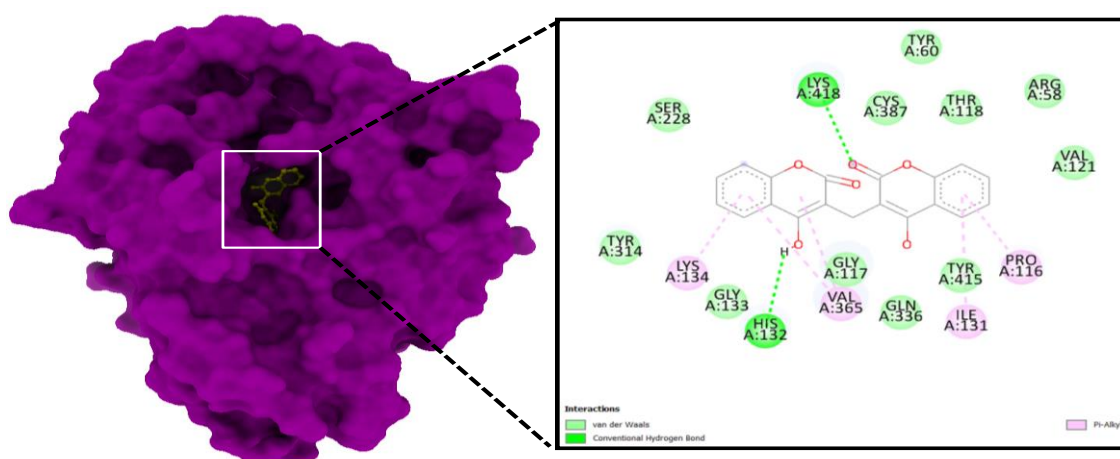


**Figure 4.** Binding pose of docked 4FEH+ compound (f) complex. A left panel displays the molecular surface of 4FEH (purple) associated with compound (f) in the ball and stick model (yellow). A right panel displays (f) 2D interaction at the binding cavity in the wireframe.



## Molecular Dynamics Simulation

The stability and convergence of the DprE1-ligand (f) complex are investigated using molecular dynamics simulation (MD). When comparing data based on the root mean square deviation (RMSD), a simulation of 100 ns revealed stable conformation (**Figure 5A**). The RMSD of the C $\alpha$ -backbone of DprE1 bound to (f) exhibited a deviation of 0.9 Å and ligand RMSD of 2.5 Å (**Figure 5A**). The ligand-bound protein's RMSD indicated stable conformations and the least perturbations. It can therefore be inferred that the DprE1-ligand (f) is relatively stable in the complex as a result of the higher affinity of the ligand.

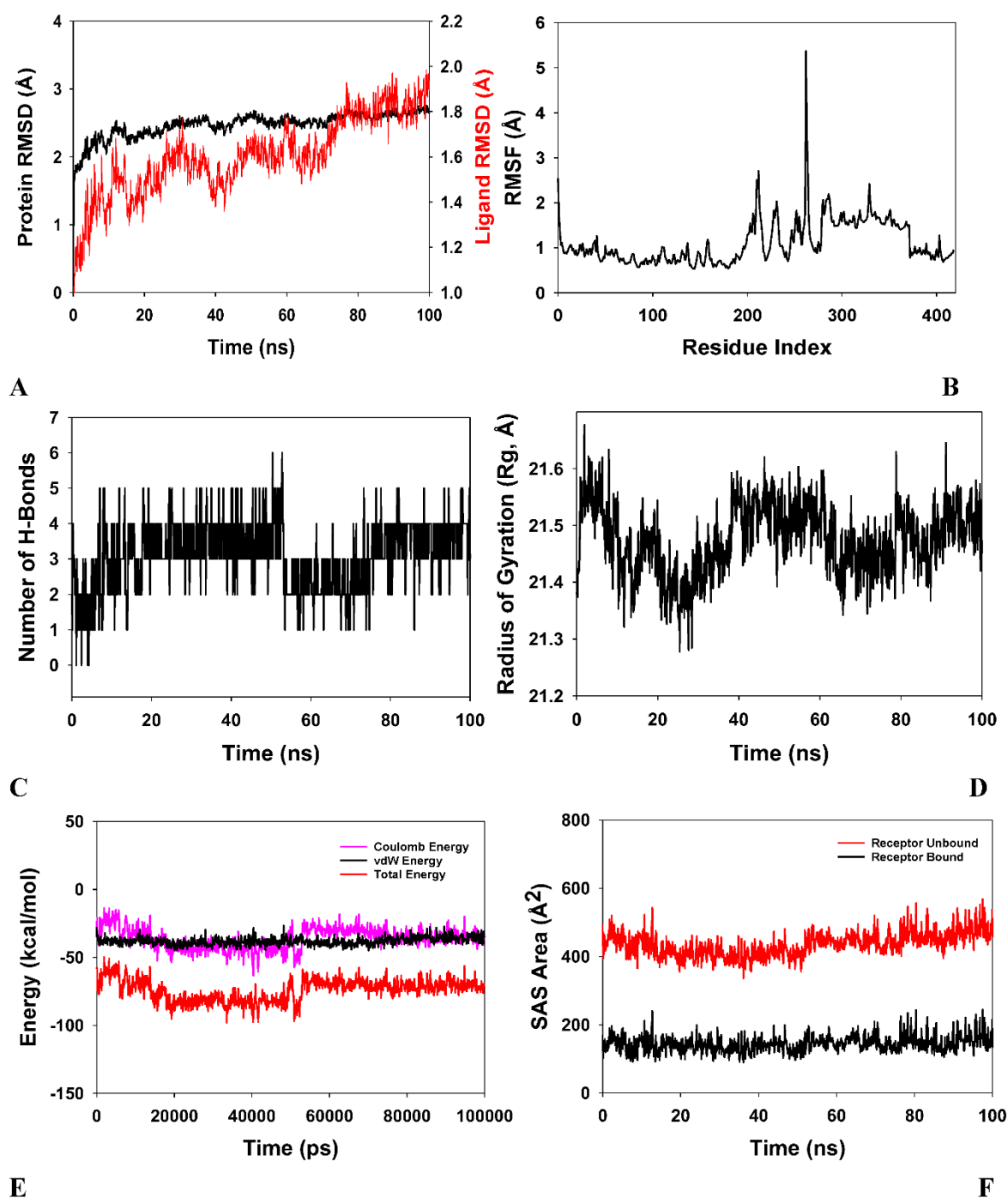


**Figure 5.** Analysis of MD simulation trajectories of 100 ns time scale. (A) RMSD plot displaying the molecular vibration of C $\alpha$  backbone of DprE1-compound (f). (B) RMSF plots show the fluctuations of respective amino acids throughout the simulation time of 100 ns for DprE1-(f). (C) Several hydrogen bonds formed between DprE1-(f) during the 100 ns simulation time scale. (D) The radius of gyration

plots for the deduction of compactness of protein DprE1-(f) Energy plots of DprE1 while complexed with ligand (E) (f). Solvent accessible surface area (SAS Area) displaying the ligand-bound (black) and unbound area (red) at the binding pocket of complex (F) DprE1-(f).

Except for amino acid residues 210 (2.6 Å) and 280 (5.7 Å) in the DprE1-ligand (f) complex, the plots for Root Mean Square Fluctuations (RMSF) showed small spikes of fluctuation, indicating that the amino-acids were in stable conformations during the simulation time (100 ns). (**Figure 5B**).

High protein residue fluctuations may be a result of loop confirmation. The number of hydrogen bonds between the ligand and the protein points to the complex's potential stability and strong interaction. During the 100 ns of simulation, a significant number of hydrogen bonds existed between DprE1 and ligand (f). (**Figure 5C**). Reliable numbers of hydrogen bonds (3 on average) are observed between DprE1 and its ligand, which could aid in forming a stable complex (**Figure 5C**). The radius of gyration quantifies the compactness of a protein. In this research, the radius of gyration (Rg) of the DprE1C $\alpha$ -backbone was found to be reduced and stable from 21.55 Å to 21.5 Å when bound to the ligand (**Figure 5D**). Stable and decreasing Rg values indicate that protein-ligand complexes are compact. It was determined from the energy profiles of DprE1-ligand systems that the entire system is stable. (**Figure 5E**) shows that the total energy of the DprE1-ligand system is very stable, with an average of -6.5 kcal/mol. However, the coulombic interaction energy seemed to be stronger than van der Waal's, with an average energy of -48 kcal/mol, contemplated as a principal contributor to the stability of the DprE1-ligand complex (**Figure 5E**). The high negative values represent the lowest potential energy in the individual systems to reach the global minima of DprE1-ligand complexes. Similar patterns in the Solvent Accessible Surface Area (SASA) in both the ligand-bound and unbound states were observed following Rg analysis. The DprE1-ligand in its unbound exhibited a substantial Solvent-Accessible Surface Area (**Figure 5F**, red), but binding with ligand (f) resulted in a lower SASA value than the unbound state (**Figure 5F**, red, black).

#### 4. Discussion

The development of antibiotics against tuberculosis infection has been complicated as most of the strains of *Mtb* become resistant to already-known antibiotics that were once effective against these strains. Other bacterial diseases that emerged later than tuberculosis no longer exist due to the development of effective antibiotics against these strains [37]. Anti-tuberculosis regimens of the first line, such as isoniazid (INH), rifampin (RIF), and pyrazinamide (PZA), are either completely ineffective or only partially effective against other types of bacteria. Although *M. smegmatis* is a fast-growing, non-virulent mycobacterial strain, INH and RIF have shown almost no activity against it, as evidenced by their 500–1000-fold higher MIC against this strain than against *M. tuberculosis* [38]. The development of novel chemotherapeutic agents against various drug-susceptible and drug-resistant bacterial diseases, including tuberculosis, requires the discovery of biologically active new chemical entities [11,39]. Medicinal plants could be a viable option for combating tuberculosis. Natural products derived from secondary metabolites of medicinal plants and their synthetic derivatives contain a variety of fascinating therapeutic qualities, including antimycobacterial activity; thus, natural products could be a promising field for finding new anti-TB leads. Coumarin is found in several plants, including sweet woodruff, tonka bean, sweetgrass, and vanilla grass. Coumarin contains a simple structure, benzopyrone, which is linked to various reactive centers. Coumarin is a robust scaffold with exceptional biological potential that has played an essential role in medicine.

Anticancer, antioxidant, and antimicrobial properties of benzopyran-2-one ring-containing heterocycles are well reported. The benzopyran-2-one ring-carrying heterocycles have anti-inflammatory, antioxidant, antithrombotic, anticancer, antimicrobial, and anti-tubercular properties [40–47]. M Nibin Joy et al. synthesized coumarin derivatives and tested them for antimicrobial activity against bacterial strains (*P. aeruginosa*, *E. coli*, and *S. aureus*) [48]. The antimicrobial properties of these synthesized compounds were good (MIC 5–150 µg/mL). Recently, Bhagat et al. synthesized novel indolinedione-coumarin derivatives and tested the effectiveness of their antibacterial properties against a variety of bacterial strains (*M. smegmatis*, *S. enteric*, *E. coli* and *S. aureus*. [49].

Rongcui Zhong et al. 2021 synthesized amphiphilic coumarin compounds and evaluated their antibacterial activity. Godge et al. developed new coumarin analogs and tested them for anti-tubercular activity, wherein all synthetic compounds displayed good anti-tubercular potency. One of the compounds exhibited potent anti-tubercular activity against *M. tuberculosis* (H37Rv strain). The study concluded that this activity might be due to the pyrazole ring and methoxy group [50]. Samina Khan Yusufzai et al. synthesized and evaluated novel thiazolyl coumarin derivatives for their anti-tubercular activity against *M. tuberculosis* and reported that compounds exhibited activity due to the thiazolyl and lipophilic methoxy substituents [51]. Kumbar et al. developed novel coumarin Schiff bases and tested them for biological activity, finding that one of the compounds had good anti-tubercular activity against *M. tuberculosis* (H37Rv) and that this action was attributable to the presence of chloro- at the para and meta of the phenyl ring [51].

Therefore, these studies show that chemistry employs synthetic methods and analytical techniques to discover and isolate natural compounds and synthesize small molecules with diverse hydrocarbon skeletons for pre-clinical investigations [52]. To aid in the hunt for fresh anti-tuberculosis agents, a battery of 8 synthetic compounds (a-h) (**Figure 2**) were synthesized and evaluated against various strains of *M. tuberculosis*. The library contained compounds with diverse chemistries. The synthesized molecules belonging to coumarins, in general, and biscoumarins, in particular, were evaluated against different mycobacterial strains, including *Mtb H37Ra*, *Mtb H37Rv*, and *M. smegmatis* and an assortment of a gram-negative and gram-positive to assess their spectrum of activity. Indeed, the test compounds were evaluated against *Mtb H37Ra* and *Mtb H37Rv* and non-virulent mycobacterial strain *M. smegmatis*. Most compounds except (a and c) were active against *Mtb H37Ra* and *Mtb H37Rv* at varying concentrations of 16-64 µg/mL. But compounds f and d were most active against *Mtb H37Ra* and *Mtb H37Rv*. The MIC of compounds f and d against these mycobacterial strains was 16 µg/mL and 32 µg/mL, which was very interesting and significant as it was substantially close to the MIC value of standard anti-TB drugs.

Interestingly, most of the compounds were not significantly active when these compounds were tested and evaluated against the non-virulent strain of *Mycobacteria*, i.e., *smegmatis*. Even if there was some activity, it was observed to be at a higher concentration of 128 µg/mL. (**Table 2**). All the bacterial strains in the current study, both gram-negative and gram-positive, were exposed to the test chemicals at concentrations ranging from 0.25 to 128 µg/mL. Levofloxacin (LVX), a common antimicrobial drug, was employed as a control. Muller-Hinton Broth was used to determine the MIC, and the findings were read after 24 hours at 37 °C [53]. Most of the test compounds were ineffective against the majority of gram-negative bacterial strains (*Pseudomonas aeruginosa* and *Escherichia coli*), as MIC was not noticed until the highest test concentrations were used (128 µg/mL). Subsequently, the majority of the test compounds showed no activity against gram-positive bacterial strains (including primarily *Enterococcus faecalis*) up to the highest tested concentrations, 128 µg/mL, except for *Bacillus subtilis*, where chemical entities were inactive below or equal to 64 µg/mL, but moderately active in the concentration range of 64-128 µg/mL. However, one of the compounds (f) showed poor activity against *Enterococcus faecalis* in 64-128 µg/mL [53]. Therefore, as evident from our observations, it is noteworthy that the biscoumarin compounds synthesized in general and compounds f and d in particular, like standard anti-tuberculosis drugs INH, RIF, and PZA, are specifically active against *M. tuberculosis* [55].

Furthermore, several cell lines of humans, including human embryonic kidney cell line HEK (HEK-293), MCF-7, MDA-MB-231, and 4T1, were subjected to the compound under study for the evaluation of the cytotoxic potential of compounds using the MTT cell viability assay to check the toxicity of the compounds. At 50 µM, it was found that, on average, all the compounds had little impact on the four cell lines (roughly a <30% growth inhibition). At a concentration of 50 µM, compounds (b) and (f) were found to be non-toxic to all of the tested cell lines, inhibiting the growth by less than 20%. Graph Pad software (v8) was used to estimate the cell viability and cytotoxicity and plotting of graphs. (**Table 3**).

**Table 3.** The cytotoxicity profile of different compounds at 50  $\mu$ M concentration depicted as % age growth inhibition in human cell lines.

Compound	MCF-7	HEK-293	MDA-MB-231	4T1
b	5.15	6.02	13.72	7.76
d	18.91	26.36	7.456	21.73
e	14.69	24.07	22.97	32.80
f	14.13	12.75	20.46	11.13
g	27.20	18.13	29.08	30.93
h	24.95	27.92	28.33	36.48

Molecular docking of biscoumarin derivatives (a-h) with different mycobacterial drug targets was performed using Autodock vina to calculate the binding affinity and find the mycobacterial drug target with which these synthesized analogs bind and inhibit bacterial growth. The structures of the different drug targets of *Mtb* were obtained from the Protein Data Bank(PDB) and were further prepared for docking purposes using specific Auto dock tools [56]. Water molecules and the inhibitors were taken out of the protein before preparing its pdbqt file. The protein structure was then changed into a pdbqt file, an input file for the AUTOGRID program Auto dock Tools incorporated polar hydrogen atoms and assigned Koulman charges. [56].

With the lowest binding energy ( $\Delta G$  – 9.3 kcal/mol) and inhibitory concentration,  $K_i$  (0.4  $\mu$ M), (f) showed a considerable binding affinity for the DprE1 drug target of *M. tuberculosis*. During the ligand (f) interaction, His132 and Lys418 residues at the binding cavity of the protein were involved in conventional hydrogen bonding. The best compound (f) pose was considered for analyzing the interactions between DprE1 and the inhibitor. The stability and convergence of the DprE1-ligand (f) complex were investigated using molecular dynamics simulation (MD). Since M D simulation can analyze the physical motions of atoms, it has become an essential tool for computer-aided drug design (CADD). M D simulation is used to assess drug candidates' stability in relation to the protein of interest.[58]. Our lead compound with the lowest MIC value, i.e., compound (f), underwent MD simulation and was validated via RMSD, RMSF, and Rg values and calculated hydrogen bonds. However, more in vivo experiments are needed because it could take many years of clinical trials before these compounds are proven to be effective drugs and made available to people.

## 5. Conclusion

In conclusion, the present study reports syntheses of a library of eight (a-h) biscoumarins and evaluates their anti-tuberculosis propensity against *M. tuberculosis* strains. Owing to their medicinal importance, Biscoumarins (a-h) were synthesized in good to excellent yield using conventional refluxing and domestic and scientific programmable microwave synthesizers. These compounds showed exceptional activity against the H37Rv, H37Ra, and *M. smegmatis* strains. Six synthesized compounds (b, d-h) showed MIC values ranging between 16-64 $\mu$ g/mL, among which the MIC value of compounds (f) and (d) is closer to the MIC of commercially available anti-tubercular drugs pyrazinamide, ciprofloxacin, and streptomycin. This study more specifically identified (f) and (d) as potential lead molecules. Cytotoxicity and molecular docking studies revealed that the activity of the compound (f) is highly selective against *M. tuberculosis* and its specific protein DprE1 compared to other microbes. On human cell lines, compound (f) was shown to be non-toxic. To the best of our knowledge, this study identified a novel chemical compound that could be a future drug candidate for TB. Thus, Biscoumarin derivatives can be promising scaffolds against *M. tuberculosis* strains and exciting systems for TB-resistant drug development.

**Author Contributions:** M.A.M and B.A.S conceptualization/design of the research work and data analysis. B.A.S. and B.A.B HZ collected the data and wrote the manuscript. M.A.M, B.A.S, B.A.B, M.A.R, and Z.A. reviewed and edited the manuscript, drew the figures/tables, and approved the final version of the manuscript. All authors have read and agreed to the published version of the manuscript.

**Funding:** This work was financially supported by grants to MAM by the Science and Engineering Research Board, Department of Science and Technology (SERB-DST) Govt. of India, New Delhi, vide Project Grant No: TAR/001213/2018.

**Conflicts of Interest:** The Author(s) declare(s) that there is no conflict of interest.

**Orcid ID:** Bashir A Sheikh:0000-0002-1087-564X; Basharat A Bhat:0000-0002-4847-4825; Masood A Rizvi: 0000-0003-0470-6329; Zahoor Ahmad:0000-0001-5694-9600; Manzoor A Mir: 0000-0003-3297-1402

## References

1. Khabibullina NF, Kutuzova DM, Burmistrova IA and Lyadova IV (2022) The biological and clinical aspects of a latent tuberculosis infection. *Tropical Medicine and Infectious Disease* 7:48.
2. Sharma JB and Yadav V (2022) Tuberculosis in Pregnancy. *Infections and Pregnancy*, Springer, pp. 63-81
3. Dartois VA and Rubin EJ (2022) Anti-tuberculosis treatment strategies and drug development: challenges and priorities. *Nature Reviews Microbiology*:1-17.
4. Rewari BB, Kumar A, Mandal PP and Puri AK (2021) HIV TB coinfection-perspectives from India. *Expert review of respiratory medicine* 15:911-930.
5. Mir MA, Hamdani SS and Qadri H (2022) Significance of immunotherapy for human bacterial diseases and antibacterial drug discovery. *Journal: Human Pathogenic Microbes*:129-161.
6. Mir MA, Albaradeh R and Agrewala JN (2013) innate-effector immune response elicitation against tuberculosis through anti-b7-1 (cd80) and anti-b7-2 (cd86) signaling in macrophages. *Ijbpas*,
7. da Silva Leite JM, Patriota YBG, de La Roca MF and Soares-Sobrinho JL (2022) New Perspectives in Drug Delivery Systems for the Treatment of Tuberculosis. *Current Medicinal Chemistry* 29:1936-1958.
8. Sheikh BA, Bhat BA, Alshehri B, Mir RA, Mir WR, Parry ZA and Mir MA (2021) Nano-drug delivery systems: Possible end to the rising threats of tuberculosis. *Journal of Biomedical Nanotechnology* 17:2298-2318.
9. Adeniji AA, Knoll KE and Loots DT (2020) Potential anti-TB investigational compounds and drugs with repurposing potential in TB therapy: a conspectus. *Applied microbiology and biotechnology* 104:5633-5662.
10. Sheikh BA, Bhat BA, Ahmad Z and Mir MA (2022) Strategies Employed to Evade the Host Immune Response and the Mechanism of Drug Resistance in Mycobacterium tuberculosis: In Search of Finding New Targets. *Current Pharmaceutical Biotechnology*.
11. Qadri H, Shah AH and Mir M (2021) Novel strategies to combat the emerging drug resistance in human pathogenic microbes. *Current Drug Targets* 22:1424-1436.
12. Watroly MN, Sekar M, Fuloria S, Gan SH, Jeyabalan S, Wu YS, Subramaniyan V, Sathasivam KV, Ravi S and Rani NNIM (2021) Chemistry, Biosynthesis, Physicochemical and Biological Properties of Rubiadin: A Promising Natural Anthraquinone for New Drug Discovery and Development. *Drug design, development and therapy* 15:4527.
13. Bhat BA, Mir WR, Sheikh BA, Rather MA and Mir MA (2022) In vitro and in silico evaluation of antimicrobial properties of Delphinium cashmerianum L., a medicinal herb growing in Kashmir, India. *Journal of Ethnopharmacology* 291:115046.
14. Sheikh BA, Bhat BA, Mehraj U, Mir W, Hamadani S and Mir MA (2021) Development of new therapeutics to meet the current challenge of drug resistant tuberculosis. *Current pharmaceutical biotechnology* 22:480-500.
15. Mir MA, Mir B, Kumawat M, Alkhanani M and Jan U (2022) Manipulation and exploitation of host immune system by pathogenic Mycobacterium tuberculosis for its advantage. *Future Microbiology* 17:1171-1198.
16. Najmi A, Javed SA, Al Bratty M and Alhazmi HA (2022) Modern approaches in the discovery and development of plant-based natural products and their analogues as potential therapeutic agents. *Molecules* 27:349.
17. Kumar M, Singh SK, Singh PP, Singh VK, Rai AC, Srivastava AK, Shukla L, Kesawat MS, Kumar Jaiswal A and Chung S-M (2021) Potential Anti-Mycobacterium tuberculosis Activity of Plant Secondary Metabolites: Insight with Molecular Docking Interactions. *Antioxidants* 10:1990.
18. Salehian F, Nadri H, Jalili-Baleh L, Youseftabar-Miri L, Bukhari SNA, Foroumadi A, Küçükkinç TT, Sharifzadeh M and Khoobi M (2021) A review: Biologically active 3, 4-heterocycle-fused coumarins. *European Journal of Medicinal Chemistry* 212:113034.



19. Mir MA, Usman M, Qadri H and Aisha S (2022) Recent trends in the development of bacterial and fungal vaccines. *Journal: Human Pathogenic Microbes*:233-259.
20. Pereira TM, Franco DP, Vitorio F and Kummerle AE (2018) Coumarin compounds in medicinal chemistry: some important examples from the last years. *Current topics in medicinal chemistry* 18:124-148.
21. Kulasari S, Singh MF and Bhandari S (2019) Polyphenols: Phytochemistry and health benefits. *J. Pharmacogn. Phytochem* 8:3344-3358.
22. Xu Z, Chen Q, Zhang Y and Liang C (2021) Coumarin-based derivatives with potential anti-HIV activity. *Fitoterapia* 150:104863.
23. Pasricha S and Gahlot P (2020) Synthetic Strategies and Biological Potential of Coumarin-Chalcone Hybrids: A New Dimension to Drug Design. *Current Organic Chemistry* 24:402-438.
24. Annunziata F, Pinna C, Dallavalle S, Tamborini L and Pinto A (2020) An overview of coumarin as a versatile and readily accessible scaffold with broad-ranging biological activities. *International Journal of Molecular Sciences* 21:4618.
25. Banday SM, Amin A, Bashir S, Qadri RA, Khan KZ and Rizvi MA (2017) Anti-metastatic propensity of biscoumarin scaffold synthesized under catalyst free aqueous phase microwave irradiation. *Croatica Chemica Acta* 90:471-481.
26. Hussain A, Rather MA, Bhat ZS, Majeed A, Maqbool M, Shah AM, Aga MA, Shah A, Mushtaq S and Sangwan PL (2019) In vitro evaluation of dinactin, a potent microbial metabolite against *Mycobacterium tuberculosis*. *International journal of antimicrobial agents* 53:49-53.
27. Moradipoodeh B, Jamalana M, Zeinali M, Fereidoonhezad M and Mohammadzadeh G (2019) In vitro and in silico anticancer activity of amygdalin on the SK-BR-3 human breast cancer cell line. *Molecular Biology Reports* 46:6361-6370.
28. Abraham CS, Muthu S, Prasana JC, Armaković SJ, Armaković S and As BG (2018) Spectroscopic profiling (FT-IR, FT-Raman, NMR and UV-Vis), autoxidation mechanism (H-BDE) and molecular docking investigation of 3-(4-chlorophenyl)-N, N-dimethyl-3-pyridin-2-ylpropan-1-amine by DFT/TD-DFT and molecular dynamics: A potential SSRI drug. *Computational Biology and Chemistry* 77:131-145.
29. Shree P, Mishra P, Selvaraj C, Singh SK, Chaube R, Garg N and Tripathi YB (2022) Targeting COVID-19 (SARS-CoV-2) main protease through active phytochemicals of ayurvedic medicinal plants—*Withania somnifera* (Ashwagandha), *Tinospora cordifolia* (Giloy) and *Ocimum sanctum* (Tulsi)—a molecular docking study. *Journal of Biomolecular Structure and Dynamics* 40:190-203.
30. Zhang C-H, Stone EA, Deshmukh M, Ippolito JA, Ghahremanpour MM, Tirado-Rives J, Spasov KA, Zhang S, Takeo Y and Kudalkar SN (2021) Potent noncovalent inhibitors of the main protease of SARS-CoV-2 from molecular sculpting of the drug perampanel guided by free energy perturbation calculations. *ACS central science* 7:467-475.
31. Bhadresha K, Upadhyay V, Kumar SP, Pandya P, Jain N and Rawal RM (2021) Computational investigation of ginkgetin and theaflavin as potential inhibitors of heat shock protein 90 (Hsp90). *Journal of Biomolecular Structure and Dynamics*:1-7.
32. Al-Otaibi JS, Mary YS, Mary S, Trivedi R, Chakraborty B, Yadav R, Celik I and Soman S (2022) DFT and MD investigations of the biomolecules of phenothiazine derivatives: interactions with gold and water molecules and investigations in search of effective drug for SARS-CoV-2. *Journal of Biomolecular Structure and Dynamics*:1-12.
33. Mukne A, Momin M, Betkar P, Rane T and Valecha S (2021) Cell-Based Assays in Natural Product-Based Drug Discovery. *Evidence Based Validation of Traditional Medicines*, Springer, pp. 211-248
34. Ferraz CAN, Tintino SR, Teixeira AMR, Bandeira PN, Santos HS, Cruz BG, Nogueira CES, Moura TF, Pereira RLS and Sena Jr DM (2020) Potentiation of antibiotic activity by chalcone (E)-1-(4'-aminophenyl)-3-(furan-2-yl)-prop-2-en-1-one against gram-positive and gram-negative MDR strains. *Microbial Pathogenesis* 148:104453.
35. Alsayed SSR, Lun S, Payne A, Bishai WR and Gunosewoyo H (2021) Design, synthesis and antimycobacterial evaluation of novel adamantane and adamantanol analogues effective against drug-resistant tuberculosis. *Bioorganic chemistry* 106:104486.
36. Mir MA (2022) *Human Pathogenic Microbes: Diseases and Concerns*. Elsevier.
37. Parameshwarappa G, Lingamani J, Patil SB and Goudgaon NM (2009) Synthesis and anti-microbial activity of thiazole substituted coumarins. *Heterocyclic Communications* 15:343-348.

38. Patil SB (2022) Medicinal significance of novel coumarin analogs: Recent studies. *Results in Chemistry* 4:100313.
39. Phutdhawong W, Chuenchid A, Taechowisan T, Sirirak J and Phutdhawong WS (2021) Synthesis and biological activity evaluation of coumarin-3-carboxamide derivatives. *Molecules* 26:1653.
40. Coronado L, Zhang X-Q, Dorta D, Escala N, Pineda LM, Ng MG, Del Olmo E, Wang C-Y, Gu Y-C and Shao C-L (2021) Semisynthesis, antiparasitic activity, and mechanism of action studies of isocoumarin derivatives. *Journal of Natural Products* 84:1434-1441.
41. Sahar A, Khan ZA, Ahmad M, Zahoor AF, Mansha A and Iqbal A (2017) Synthesis and antioxidant potential of some biscoumarin derivatives. *Tropical Journal of Pharmaceutical Research* 16:203-210.
42. Joy MN, Bakulev VA, Bodke YD and Telkar S (2020) Synthesis of coumarins coupled with benzamides as potent antimicrobial agents. *Pharmaceutical Chemistry Journal* 54:604-621.
43. Mk BKBG (2019) Singh JV Gulati HK Singh A. Kaur K. Kaur G. Sharma S. Rana K. Singh H. Sharma S. Singh Bedi PM *ACS Omega* 4:8720-8730.
44. Godge R and Kunkulol R (2018) Synthesis of Coumarin heterocyclic derivatives with In-Vitro antitubercular activity. *Journal of Drug Delivery and Therapeutics* 8:217-223.
45. KhanYusufzai S, Osman H, Khan MS, Mohamad S, Sulaiman O, Parumasivam T, Gansau JA and Johansah N (2017) Design, characterization, in vitro antibacterial, anti-tubercular evaluation and structure–activity relationships of new hydrazinyl thiazolyl coumarin derivatives. *Medicinal Chemistry Research* 26:1139-1148.
46. Pollo LAE, Martin EF, Machado VR, Cantillon D, Wildner LM, Bazzo ML, Waddell SJ, Biavatti MW and Sandjo LP (2021) Search for antimicrobial activity among fifty-two natural and synthetic compounds identifies anthraquinone and polyacetylene classes that inhibit *Mycobacterium tuberculosis*. *Frontiers in Microbiology*:3619.
47. Rather MA, Lone AM, Teli B, Bhat ZS, Singh P, Maqbool M, Shaingojoy BA, Dar MJ, Amin S and Yousuf SK (2017) The synthesis, biological evaluation and structure–activity relationship of 2-phenylaminomethylene-cyclohexane-1, 3-diones as specific anti-tuberculosis agents. *MedChemComm* 8:2133-2141.
48. Acharya P, Ramana MMV, Upadhyay M and Pavale G (2021) Unveiling the Anti-tubercular Properties of Biscoumarins, through Biological Evaluation and Docking Studies. *Letters in Drug Design & Discovery* 18:57-66.
49. Qasaymeh RM, Rotondo D, Oosthuizen CB, Lall N and Seidel V (2019) Predictive binding affinity of plant-derived natural products towards the protein kinase g enzyme of *mycobacterium tuberculosis* (mtpkng). *Plants* 8:477.
50. Aljahdali MO, Molla MHR and Ahammad F (2022) Immunoinformatics and Computer-Aided Drug Design as New Approaches against Emerging and Re-Emerging Infectious Diseases.

**Disclaimer/Publisher's Note:** The statements, opinions and data contained in all publications are solely those of the individual author(s) and contributor(s) and not of MDPI and/or the editor(s). MDPI and/or the editor(s) disclaim responsibility for any injury to people or property resulting from any ideas, methods, instructions or products referred to in the content.